

# Superoxide Generation in v-Ha-ras-Transduced Human Keratinocyte HaCaT Cells

Ji-Qin Yang, Shijun Li, Frederick E. Domann, Garry R. Buettner, and Larry W. Oberley\*

Radiation Research Laboratory, Department of Radiology, The University of Iowa, Iowa City, Iowa

The oncogenic ras protein controls signal-transduction pathways that are critical for cell proliferation and tumorigenesis. Here, we demonstrate that v-Ha-ras-transduced human keratinocyte HaCaT cells produced significantly larger amounts of superoxide than did control cell lines. The superoxide generation was mediated by the transduced ras protein, because superoxide generation was modified by an inhibitor, lovastatin, that inhibits ras farnesylation during ras protein maturation. Superoxide generation was also inhibited by diphenylene iodonium, an inhibitor of flavoproteins, including NADPH oxidase, but not by rotenone, an inhibitor of the respiratory chain of the mitochondria. Those observations suggested that a phagocytic-like NADPH oxidase exists in keratinocytes that could be activated by the dominant activated v-Ha-ras and produce superoxide. Overexpression of manganese-containing superoxide dismutase and copper and zinc-containing superoxide dismutase cDNA via adenovirus infection also attenuated superoxide generation. Previous work has demonstrated that extracellular superoxide dismutase (SOD) can lower superoxide generation; this is the first report that intracellular SOD could also modify the amount of superoxide production from the cells. This report implies that superoxide radical may act as a second messenger molecule of oncogenic ras. *Mol. Carcinog.* 26:180–188, 1999. © 1999 Wiley-Liss, Inc.

**Key words:** manganese-containing superoxide dismutase; catalase; free radical; reactive oxygen species

## INTRODUCTION

Reactive oxygen species (ROS) are oxygen-containing species that have chemical reactivity greater than ground-state dioxygen. ROS include superoxide radical ( $O_2^{\cdot-}$ ), hydroxyl radical ( $\cdot OH$ ), singlet oxygen ( $^1O_2$ ), and hydrogen peroxide ( $H_2O_2$ ). Superoxide and its reaction products produced within the cell can damage cellular components, particularly the metabolic enzymes, membranes, and DNA. Superoxide is generated during the process of normal aerobic metabolism and rapidly dismutates either spontaneously or enzymatically, forming  $H_2O_2$  and  $O_2$ .

Phagocytes can produce a large amount of superoxide through a specific enzyme system, NADPH oxidase [1,2]. When white cells are activated, the enzyme's cytosolic components are able to assemble, and the membrane components form a functional complex. Electrons are then transferred from NADPH to molecular oxygen with the subsequent generation of superoxide anion [1,2]. It is thought that a similar NADPH oxidase exists in some nonleukocytic cells, and when there is stimulation, this enzyme can also generate superoxide radicals. A number of non-leukocytic cell types, including fibroblasts, smooth muscle cells, endothelial cells, keratinocytes, and mesangial cells, generate low levels of superoxide but when activated can also produce much more superoxide [3–6].

During evolution, aerobic cells have developed a complex antioxidant enzyme system to control the levels of  $O_2^{\cdot-}$  and other ROS molecules; this system

includes manganese-containing superoxide dismutase (MnSOD), copper and zinc-containing superoxide dismutase (CuZnSOD), catalase (CAT), and glutathione peroxidase (GPx) [7]. Both MnSOD and CuZnSOD, which are found in the mitochondria and the cytosol, respectively, scavenge superoxide and generate hydrogen peroxide, whereas CAT and GPx convert  $H_2O_2$  into water. In this way, two toxic species,  $O_2^{\cdot-}$  and  $H_2O_2$ , are converted into harmless water. In oxygen-metabolizing cells, the superoxide dismutase (SOD) enzymes are regarded as necessary for life; either mutation or deficiency can cause serious diseases in humans. In normal conditions, the steady-state concentrations of  $O_2^{\cdot-}$  and  $H_2O_2$  may greatly influence cellular redox potential. A growing body of evidence suggests that cellular redox potential may regulate signal transduction [5,8–10]. In mammalian cells, a variety of extracellular stimuli, including cytokines and growth

\*Correspondence to: Radiation Research Laboratory, B180 Medical Laboratories, Department of Radiology, The University of Iowa, Iowa City, Iowa 52242.

Received 13 April 1999; Revised 12 July 1999; Accepted 20 July 1999

Abbreviations: ROS, reactive oxygen species; MnSOD, manganese-containing superoxide dismutase; CuZnSOD, copper and zinc-containing superoxide dismutase; CAT, catalase; GPx, glutathione peroxidase; SOD, superoxide dismutase; RT, reverse transcription; PCR, polymerase chain reaction; GAPDH, glyceraldehyde-3-phosphate dehydrogenase; DMPO, 5,5-dimethyl-1-pyrroline-N-oxide; EPR, electron paramagnetic resonance; AdMnSOD, adenovirus-MnSOD construct; AdCuZnSOD, adenovirus-CuZnSOD construct; AdCAT, adenovirus-CAT construct; AdlacZ, adenovirus-lacZ construct; SD, standard deviation; DPI, diphenylene iodonium; NBT, nitroblue tetrazolium.

factors, produce a transient burst of ROS [8,9]. Inhibition of this rise in intracellular ROS by either chemical or enzymatic scavengers has been shown to inhibit platelet-derived growth factor-stimulated signal transduction [8] as well as cytokine-stimulated gene transcription [9].

The *ras* family of proto-oncogenes encodes small GTP-binding proteins that transduce mitogenic signals from the tyrosine-kinase receptors [11]. *ras* is a 21-kDa membrane-anchored protein. Amplification of *ras* proto-oncogenes and mutations that constitutively activate *ras* proteins are frequent in human bladder, lung, and colon carcinomas [12]. v-Ha-*ras*, which is mutated in amino acids 12 and 59, is a kind of dominant activated *ras* [12]. Previous experiments have shown that mutant *ras*-transduced fibroblasts can generate  $O_2^-$  by a pathway involving a fibroblast-type NADPH oxidase, and the  $O_2^-$  generated may act as a second messenger molecule to promote cell proliferation [5]. Based on the previous evidence linking *ras* to superoxide production in fibroblasts, in this study we explored the possibility that v-Ha-*ras* expression induces superoxide generation and *ras* phenotypes in human keratinocyte HaCaT cells and examined the relationship between the superoxide production and the levels of intracellular antioxidant enzymes. We demonstrate for the first time that elevation of intracellular superoxide dismutase (SOD) reduces the levels of superoxide radicals induced by over-expression of v-Ha-*ras*.

## MATERIALS AND METHODS

### Cell Culture

The HaCaT cell line (a gift from Professor N. Fusenig, Institute of Biochemistry, German Cancer Research Center, Heidelberg, Germany) was derived from human keratinocytes spontaneously immortalized in vitro during long-term incubation of a primary culture under selected culture conditions [13]. D19 was one of several v-Ha-*ras* cDNA-transduced HaCaT clones in which the total Ha-*ras* protein levels were increased dramatically. The cultures were maintained at 37°C in 5% CO<sub>2</sub> and Dulbecco's modified Eagle's medium (with high glucose (4.5 g/L)) supplemented with 10% heat-inactivated fetal bovine serum and antibiotics (100 U/mL penicillin and 100 µg/mL streptomycin).

### v-Ha-*ras* cDNA Transfer

The v-Ha-*ras*-encoding plasmid pLNL6 (a gift from Dr. M. N. Gould, University of Wisconsin, Madison, WI) was used as the vector to generate stably transfected cell lines [14]. The v-Ha-*ras* gene was driven by a retrovirus long terminal repeat promoter, and the neomycin-resistance gene was governed by an internal simian virus 40 early promoter to provide a selection marker. HaCaT cells

( $1 \times 10^6$ ) were seeded in six-well plates and allowed to grow for 24 h. The medium was removed, and the cells were transfected with 2 µg of the v-Ha-*ras* pLNL6 construct and 10 µL of Lipofectamine (Life Technologies, Gaithersburg, MD) as vehicle per dish. Selection for neomycin-resistant cells (with geneticin G418, 800 µg/mL) started 24 h after passaging. The cells were refed twice a week with the medium listed above, and individual colonies were removed by ring isolation from different parent dishes. For propagation, the cells were maintained in medium containing G418 (400 µg/mL). The G418 was removed 3 d before each experiment.

### Western Blotting Analysis

Cells were harvested and lysed by sonication and then separated by 12.5% sodium dodecyl sulfate-polyacrylamide gel electrophoresis. The proteins were electrotransferred to nitrocellulose sheets. After blocking in 5% milk for 30 min, the sheets were washed and treated with antisera to MnSOD (diluted 1:1000), CuZnSOD (diluted 1:1000), or CAT (diluted 1:1000) or monoclonal antibody to pan-Ha-*ras* (Oncogene Science Inc., Uniondale, NY; diluted 1:1000) for 30 min. Polyclonal rabbit antibodies to human MnSOD, CuZnSOD, and CAT have been prepared and characterized in our laboratory [15]. The blots were incubated with horseradish peroxidase-conjugated goat anti-rabbit immunoglobulin G (Sigma Chemical Co. St Louis, MO; diluted 1:10 000) for 1 h at room temperature. The washed blots were then treated with ECL western blot detection solution (Amersham Life Science, Buckinghamshire, UK) and exposed to X-ray film.

### Reverse Transcription-Polymerase Chain Reaction Assay

One microgram of total RNA was used for the reverse transcription (RT) reaction to make cDNA from all mRNA. The sense primer sequence for c-Ha-*ras* cDNA was 5'-ACACACTTGACAGCTCATGCA-3', and the antisense primer sequence was 5'-GACAGAATACAAGCTTGTGG-3'. This primer pair was predicted to produce a 554-bp DNA fragment. For amplification of cDNA, 1 µL of RT product was mixed with 5 µL of 10 × polymerase chain reaction (PCR) buffer, 1 µL of 200 µM dNTP, 0.5 µL of 0.1 µM of sense primer, 0.5 µL of 0.1 µM of antisense primer, and 2.5 U of Taq polymerase (Boehringer Corp., Mannheim, Germany). The PCR was performed for 30 cycles. For normalization, parallel samples were amplified with primers designed for a housekeeping gene, glyceraldehyde-3-phosphate dehydrogenase (*GAPDH*). The primers used were sense primer 5'-AAGGTCATCCATGACAAC-3' and antisense primer 5'-GCTTCACCACCTTCTTGATG-3', which were predicted to produce a 307-bp product. One microliter of RT reaction was used for the *GAPDH* PCR reaction. The other conditions were as described

above. Ten microliters of PCR product was loaded and run on a 1.5% agarose gel.

### 5,5-Dimethyl-1-pyrroline N-oxide Spin Trapping of Superoxide Radicals

5,5-Dimethyl-1-pyrroline N-oxide (DMPO) was prepared in Krebs-Ringer buffer, pH 7.4. The buffer was passed through a Chelex-100 ion exchange column (Bio-Rad, Inc., Richmond, CA) to remove trace metal impurities [16]. EDTA (0.1 mM) was added to sequester further any residual trace metal ions. Cells were seeded in six-well plates. The medium was then removed, and the cells were washed twice in Krebs-Ringer buffer. The cells were incubated with 100 mM DMPO (final concentration) at 37°C and 5% CO<sub>2</sub> for 5 min, and then samples were placed in an electron paramagnetic resonance (EPR) spectrometer. The EPR spectra of the DMPO adducts were recorded with a Bruker ESP300 EPR spectrometer equipped with a TM<sub>110</sub> cavity (Bruker Instrument, Karlsruhe, Germany).

### Cytochrome c Assay for Superoxide Generation

The production of superoxide was measured by its reduction of cytochrome c [17]. Cells were cultured in six-well plates. The medium was then removed, and the cells were washed twice in Krebs-Ringer buffer. Cytochrome c (100 μM) in Krebs-Ringer buffer with CAT (200 U/mL) was added to the wells, and samples were removed after 1 h of incubation at 37°C in 5% CO<sub>2</sub>. The spectrum of each sample between 400 and 600 nm was then assessed. Superoxide production was determined by measuring the peak height at 550 nm over the baseline between 530 and 560 nm. CAT was present in the cytochrome c solution because of concern that H<sub>2</sub>O<sub>2</sub> produced by the cells could re-oxidize the reduced cytochrome c. The extinction coefficient  $\epsilon = 2.99 \times 10^4$  M/cm was used to calculate reduced cytochrome c concentration [17].

### Adenovirus Gene Transfer

The adenovirus constructs used were replication-defective, E1-deleted recombinant adenoviruses [18]. Human *MnSOD* cDNA, human *CuZnSOD* cDNA, human *CAT* cDNA, or *lacZ* cDNA was inserted into the E1 region of the viral genome, and these foreign genes were driven by a cytomegalovirus promoter [19]. Approximately  $2 \times 10^5$  D19 cells were seeded in six-well plates and left to adhere for 12 h. The cells were then washed three times in serum-free medium. The adenovirus-*MnSOD* (Ad*MnSOD*), adenovirus-*CuZnSOD* (Ad*CuZnSOD*), and adenovirus-*CAT* (Ad*CAT*) constructs were added to cells in 2 mL of serum-free medium at MOIs of 50 or 100. Control cells were treated with the adenovirus-*lacZ* (Ad*LacZ*) construct at an MOI of 100. The cells were incubated with adenovirus constructs for 24 h. Serum-free medium was re-

placed with 2 mL of complete medium for an additional 24 h before the cells were assayed for superoxide production and immunoreactive protein.

### SOD and CAT Activity Gel Assay

SOD and CAT activities were measured by using a native-gel activity stain. A 8% running gel and 5% stacking gel was used to separate the proteins. For the SOD activity stain, the gel was stained with 2.43 mM nitroblue tetrazolium (NBT) solution for 20 min and then 28 μM riboflavin with 28 mM TEMED for 15 min. The gel was placed in distilled water and illuminated under a bright fluorescent light. Achromatic bands indicated the presence of SOD. For the CAT activity stain, the gel was first rinsed three times with distilled water and then incubated in 0.003% H<sub>2</sub>O<sub>2</sub> for 10 min. The gel was then stained with 2% ferric chloride and 2% potassium ferricyanide; when achromatic bands begin to form, the stain was poured off and the gel rinsed extensively with distilled water. Achromatic bands demonstrated the presence of CAT activity. Two hundred micrograms of total protein from cell lysates was run in each lane.

### Statistical Analysis

Statistical analysis was performed with SYSTAT (Systat, Evanston, IL). A single factor analysis of variance, followed by a post hoc Tukey test, was used to determine statistical differences between means. The null hypothesis was rejected at the 0.05 level of significance. All means were calculated from three experiments, and the error bars represent standard derivations (SDs). All western blot, RT-PCR, and activity gel assays were repeated at least twice.

## RESULTS

### v-Ha-ras Overexpression in HaCaT Transfectants

Human keratinocyte HaCaT cells were stably transduced by a dominant activated ras, v-Ha-ras, through the retrovirus-encoding plasmid construct pLNL6 [14]. G418 resistant clones were selected. The ras protein level was detected by western blotting in these clones. We isolated several clones and chose to study one clone, D19, that stably expressed a higher level of v-Ha-ras than did the parental cells and Neo cells (shown in Figure 1A). There were two bands of ras protein on the western blot. As shown previously, the upper band was the mature ras that had covalent binding of polyisoprenoid after a series of post-translational modifications; the lower band was the ras that had no such modifications [20]. There was a small difference in their mobilities in sodium dodecyl sulfate-polyacrylamide gels.

RT-PCR showed that the v-Ha-ras gene was expressed in D19 clones. RT-PCR was performed to

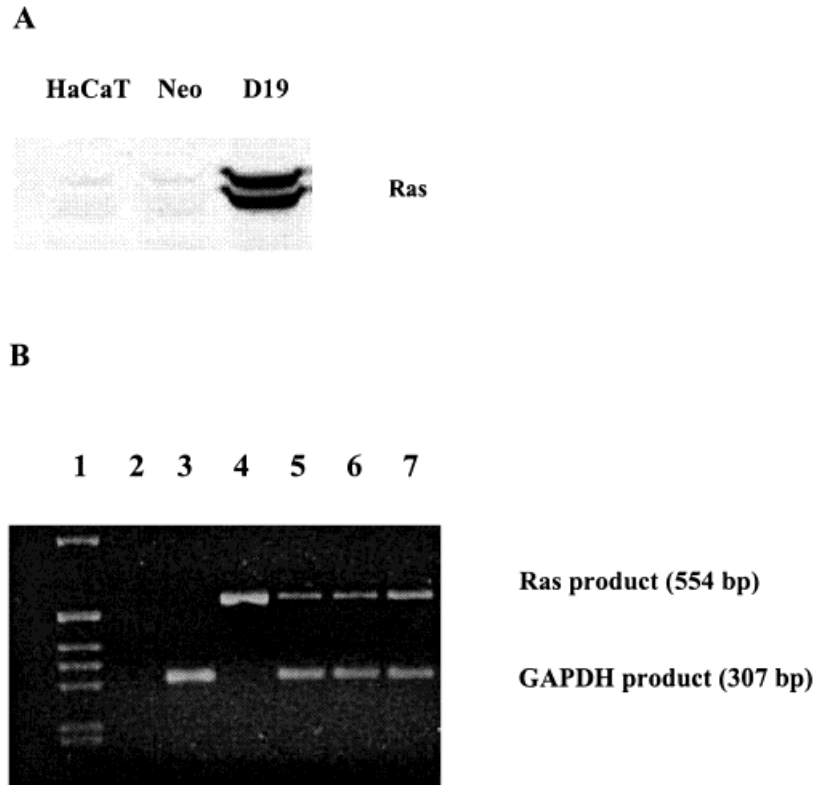


Figure 1. v-Ha-ras overexpression in HaCaT transfectants. (A) Western blotting analysis of pan-ras. Cell lysates (100  $\mu$ g) were run on a 12.5% sodium dodecyl sulfate–polyacrylamide gel, and the proteins were electrotransferred to nitrocellulose sheets. The sheets were treated with mouse monoclonal antibody against pan-Ha-ras. D19 is a v-Ha-ras–transduced clone, Neo is a vector-transduced clone, and HaCaT is the parental line. Increased ras protein was shown in D19 cells. (B) RT-PCR for *ras* gene transcription. Total RNA

(1  $\mu$ g) was used for RT to synthesize cDNA, and 1  $\mu$ L of RT product was used for PCR. The primers for *ras* produced a 554-bp product. The PCR was performed for 30 cycles. A parallel RT-PCR was conducted with *GAPDH* primers, which produced a 307-bp product. The PCR products were loaded and run on a 1.5% agarose gel. Lane 1, 1-kb DNA ladder; lane 2, blank control; lane 3, *GAPDH* positive control; lane 4, *ras* cDNA positive control; lane 5, HaCaT; lane 6, Neo; lane 7, D19. Increased *ras* mRNA was seen in D19 cells.

study the quantity of *ras* mRNA. One microgram total RNA was reverse transcribed to obtain cDNA from mRNA. By PCR, a 554-bp fragment was generated from a pair of *ras*-specific primers (Figure 1B). We also performed a parallel RT-PCR for *GAPDH* mRNA at the same time to monitor the variation in total RNA amount. The *GAPDH* RT-PCR product was about 307 bp. Figure 1B clearly shows that the 554-bp *ras* PCR bands were more intense in D19 cells (lane 7) than in parental HaCaT cells (lane 5) and Neo cells (lane 6). The intensities of the 307-bp *GAPDH* mRNA PCR bands were all nearly the same, which means that the total RNA amounts in each lane were nearly equal. It should be noted that the increases in v-Ha-ras mRNA shown in Figure 1B are much less than the increases in ras protein shown in Figure 1A. This could be because the primers used also detected other forms of *ras* mRNA besides v-Ha-ras, or because the RT-PCR assay used was only semiquantitative. The RT-PCR results demonstrated that the v-Ha-ras gene was transcribed and processed to mature mRNA in the ras-transfected HaCaT cells.

#### ras-Mediated Superoxide Production

We used EPR spectroscopy and the spin trap DMPO to study superoxide produced in D19 cells. D19 cells displayed a 1:2:2:1 quartet signal (with  $a^H = a^N = 14.9$  G) indicative of DMPO/ $\text{HO}^\bullet$  adducts [21], whereas Neo cells and HaCaT cells generated only a weak similar signal (Figure 2). Neo produced slightly more signal than the parental line; this is probably because Neo is a clonal isolate with slightly different properties than the parental line. The DMPO/ $\text{HO}^\bullet$  adduct can be formed either by direct trapping of hydroxyl radical ( $\text{HO}^\bullet$ ) or by rapid breakdown of DMPO/ $\text{O}_2^{\bullet-}$ , formed from  $\text{O}_2^{\bullet-}$  [22]. The addition of exogenous CuZnSOD protein (450 U/mL) to intact cells almost totally inhibited the DMPO signal (Figure 2). However, the addition of CAT protein (500 U/mL) did not change the DMPO/ $\text{HO}^\bullet$  signal; this result demonstrates that  $\text{H}_2\text{O}_2$  is not an intermediate in the production of the DMPO/ $\text{HO}^\bullet$  adduct. These experiments show that the observed EPR signal is attributable to the spin trapping of  $\text{O}_2^{\bullet-}/\text{HO}_2^\bullet$  rather than to  $\text{HO}^\bullet$  derived

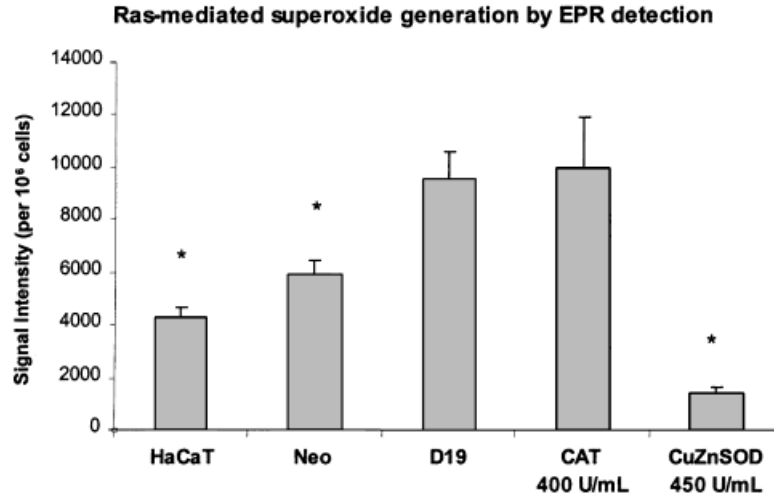


Figure 2. ras-mediated superoxide generation observed by DMPO spin trapping and EPR spectroscopy. EPR spin trapping was used to measure superoxide production in HaCaT, Neo, D19, and D19 cells further treated with CuZnSOD or CAT. The signals were recorded after incubating the cells with the 100 mM DMPO spin trap for 5 min with a Bruker ESP300 spectrometer. Cell number was determined after EPR spectroscopy. DMPO/HO<sup>•</sup> spin trap peak values per  $1 \times 10^6$

cells were determined. The conditions are indicated in Materials and Methods. Signal intensity is given in arbitrary units. Means were calculated from three experiments, and the error bars represent the SD. \*, statistically different from D19 cells at the  $P < 0.05$  level. D19 cells had increased superoxide production compared with the controls, and this was inhibited by CuZnSOD protein.

from H<sub>2</sub>O<sub>2</sub> but did not rule out the possibility that H<sub>2</sub>O<sub>2</sub> was generated within these cells, probably by the rapid dismutation of O<sub>2</sub><sup>•-</sup>. The EPR signal intensity of DMPO/HO<sup>•</sup> from D19 cells (Figure 2) was about double that from HaCaT cells.

Production of O<sub>2</sub><sup>•-</sup> was further confirmed by the cytochrome C assay, which has good specificity for O<sub>2</sub><sup>•-</sup>. Cytochrome c can be reduced by O<sub>2</sub><sup>•-</sup> from cytochrome c (Fe<sup>3+</sup>) to cytochrome c (Fe<sup>2+</sup>), with a rate constant  $k = 1.5 \times 10^5$ /M/s (ph 7–9.3) and extinction coefficient of cytochrome c (Fe<sup>2+</sup>)  $\epsilon_{m550} = 2.99 \times 10^4$ /M/cm and cytochrome c (Fe<sup>3+</sup>)

$\epsilon_{m550} = 0.89 \times 10^4$ /M/cm [17]. The cytochrome c measurements for superoxide production were consistent with the EPR measurements (Figure 3). The D19 clone generated about three times more superoxide than did the parental HaCaT cells. Cytochrome c reduction was also inhibited by the addition of SOD protein (450 U/mL). When D19 cells were treated with 80  $\mu$ M lovastatin, a drug that inhibits ras protein maturation, 2 d before measurement, superoxide generation was greatly decreased. These results support the hypothesis that mutant ras can mediate superoxide production.

### Ras mediated superoxide generation in D19 Cells

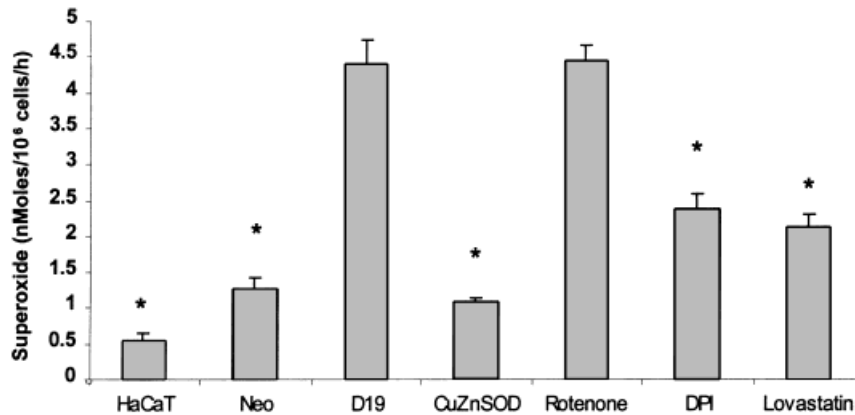
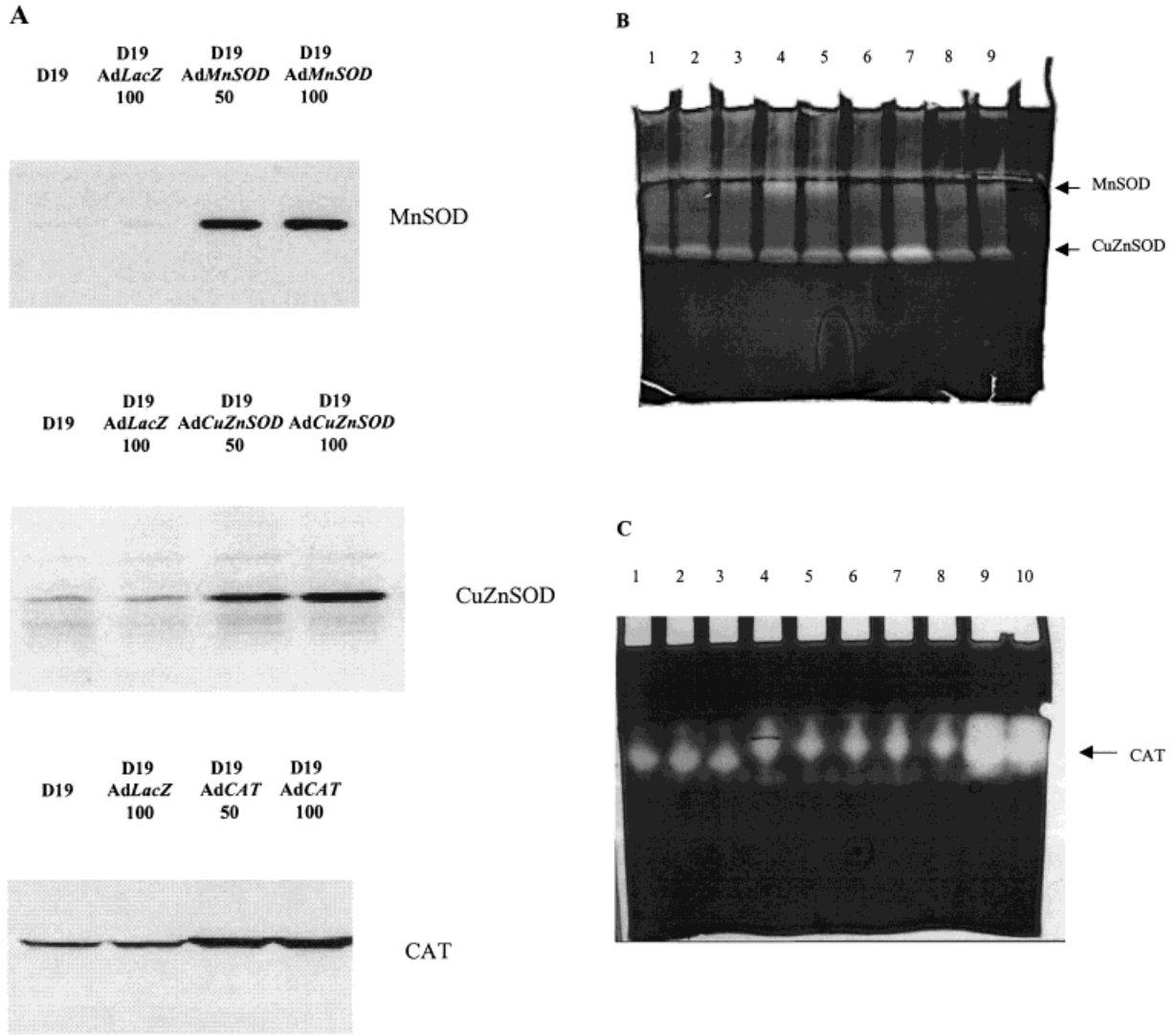


Figure 3. ras-mediated superoxide production measured by the cytochrome c assay. Cells in six-well plates were washed with Krebs-Ringer buffer and then treated with 100  $\mu$ M cytochrome c in Krebs-Ringer buffer with 200 U/mL CAT at 37°C and 5% CO<sub>2</sub> for 1 h. Samples were taken and scanned at wavelengths from 400 to 600 nm; the 550-nm peak height was measured. D19 cells were also treated with CuZnSOD (450 U/mL) 10 min before the assay or with

rotenone (100  $\mu$ M) 2 h before, DPI (100  $\mu$ M) 2 h before, or lovastatin (80  $\mu$ M) 24 h before superoxide measurement. Cell numbers were determined after the assay. Means were calculated from three experiments, and the error bars represent the SD. \*, statistically different from D19 cells at the  $P < 0.05$  level. D19 cells showed higher superoxide levels than the control cells, and the superoxide levels were lowered by CuZnSOD protein, DPI, and lovastatin.



**D**

**AdSOD transfection inhibited Ras-mediated superoxide generation**

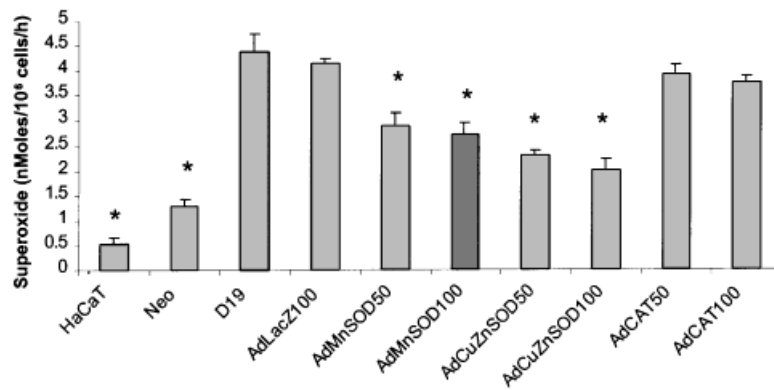


Figure 4. See legend on next page.

### Keratinocytic NADPH Oxidase Possibly Involved in ras-Mediated Superoxide Generation

Figure 3 shows that D19 cells treated with 100  $\mu$ M diphenylene iodonium (DPI), an inhibitor of flavo-proteins, including NADPH oxidase, 2 h before measuring superoxide generation had greatly decreased superoxide levels. This suggests that v-Ha-ras-induced superoxide generation is mediated by the activation of keratinocyte NADPH oxidase. However, when D19 cells were treated with 100  $\mu$ M rotenone, an inhibitor of the respiratory chain in mitochondria, for 2 h before the cytochrome c measurement, there was no inhibition. Thus, the respiratory chain of the mitochondria appears not to be the major source of the observed superoxide production.

### Modulation of ras-Mediated Superoxide Production by *MnSOD* or *CuZnSOD* cDNA Transduction

MnSOD, CuZnSOD, CAT, and GPx are important members of the cellular antioxidant enzyme family; they cooperate to protect cells from damage by ROS. To investigate whether increased intracellular MnSOD, CuZnSOD, or CAT enzyme could modify v-Ha-ras-mediated superoxide generation, we infected D19 cells with human *MnSOD*, *CuZnSOD*, and *CAT* cDNA adenovirus constructs. We used these adenovirus constructs at MOIs of 50 and 100 and also used bacterial *lacZ* gene adenovirus constructs as controls. Western blotting (Figure 4A) showed that these enzyme proteins were highly expressed 48 h after transduction. To investigate the intracellular MnSOD and CuZnSOD activity, 200  $\mu$ g of total protein samples from adenovirus construct-transduced D19 cells was run on a native activity gel. Figure 4B shows that the expressed MnSOD and CuZnSOD had high activity in an SOD activity gel. The Ad*MnSOD* (lanes 4 and 5)- and Ad*CuZnSOD* (lanes 6 and 7)-transduced D19 cells had higher activity than did D19 (lane 2) and Ad*LacZ* (lane 3)-transduced D19 cells. It should be noted that these activity gels show saturation at high SOD activities; this may explain why the MnSOD activity in lane 4

(MOI 50) was similar to that in lane 5 (MOI 100). Figure 4C shows that the expressed CAT had high activity in a CAT activity gel. The Ad*CAT*-transduced D19 cells (lanes 9 and 10) had much higher activity than the other comparable cells. Figure 4D shows the superoxide generation by the cytochrome C assay after SOD adenovirus construct transduction of D19 cells. We found that both Ad*CuZnSOD* and Ad*MnSOD* transduction attenuated superoxide generation compared with that of the D19 clone; however, Ad*CAT* transduction had no effect on superoxide generation.

### DISCUSSION

The proto-oncogene product p21<sup>ras</sup> (c-Ha-ras) participates in various cellular processes, including proliferation, differentiation, and cytoskeletal organization [11]. Overexpression of normal or mutant ras that renders it constitutively active has been described in various human tumors. However, how ras activates the downstream targets is not fully understood. Our research showed for the first time in human keratinocytes that v-Ha-ras expression led to an increase in superoxide production (previous work had been done in fibroblasts). The source of the superoxide radical appears to be a phagocytic-like NADPH oxidase located in the plasma membrane. The presence of superoxide dismutase can modify this superoxide production. Further work is necessary to verify the source of the superoxide production.

The phagocyte-NADPH oxidase or respiratory burst oxidase is a multicomponent enzyme complex and catalyzes the one-electron reduction of oxygen to superoxide. Several groups have shown that NADPH oxidase exists in non-phagocytic cells, including endothelial cells [3], fibroblasts [5], and vascular smooth muscle cells [6]. The NADPH oxidase systems in these cells have not yet been characterized. To determine whether HaCaT has an NADPH oxidase system that is involved in ras-mediated superoxide generation, we treated D19 cells with DPI and found that both the DMPO/HO<sup>•</sup> signal and cytochrome c measurements were at-

Figure 4. SOD gene transfer inhibited ras-mediated superoxide generation by the cytochrome c assay. D19 cells ( $2 \times 10^5$ ) were transiently transfected by adenovirus constructs of human *CuZnSOD*, *MnSOD*, or *CAT* genes at MOIs of 50 or 100. D19 cells transfected with an adenovirus *lacZ* gene construct (MOI 100) were used as a control. (A) Western blotting analysis of increased MnSOD, CuZnSOD, and CAT protein levels after adenovirus construct transfection. The cells were harvested after the cytochrome c assay, and the MnSOD, CuZnSOD, and CAT protein levels were measured by immunoblotting. Increased levels of the three proteins were demonstrated after adenovirus transduction. (B) SOD activity gel showing increased SOD activity in adenovirus *MnSOD* and *CuZnSOD* construct-transduced D19 cells. Protein (200  $\mu$ g) from lysed cells was separated in a native gel, and the gel was stained with NBT solution to show the MnSOD and CuZnSOD activity. Lane 1, HaCaT; lane 2, D19; lane 3, D19 Ad*LacZ* MOI 100; lane 4, D19 Ad*MnSOD* MOI 50; lane 5, D19 Ad*MnSOD* MOI 100; lane 6, D19 Ad*CuZnSOD*

MOI 50; lane 7, D19 Ad*CuZnSOD* MOI 100; lane 8, D19 Ad*CAT* MOI 50; lane 9, D19 Ad*CAT* MOI 100. (C) CAT activity gel showing increased CAT activity in Ad*CAT*-transduced D19 cells. Lane 1, HaCaT; lane 2, Neo; lane 3, D19; lane 4, D19 Ad*LacZ* MOI 100; lane 5, D19 Ad*MnSOD* MOI 50; lane 6, D19 Ad*MnSOD* MOI 100; lane 7, D19 Ad*CuZnSOD* MOI 50; lane 8, D19 Ad*CuZnSOD* MOI 100; lane 9, D19 Ad*CAT* MOI 50; lane 10, D19 Ad*CAT* MOI 100. (D) Cytochrome C assay of superoxide generation. Ad*LacZ* 100, Ad*CuZnSOD* 50, Ad*CuZnSOD* 100, Ad*MnSOD* 50, Ad*MnSOD* 100, Ad*CAT* 50, and Ad*CAT* 100 indicate that the adenovirus constructs named were transfected into D19 cells at the indicated MOIs. Means were calculated from three experiments, and the error bars represent the SD. \*, significantly different from D19 cells at the  $P < 0.05$  level. Ad*MnSOD* was not significantly different from Ad*CuZnSOD* ( $P > 0.05$ ), nor was MOI 50 different from MOI 100 ( $P > 0.05$ ) for both SOD proteins.

nuated (Figure 3). When D19 cells were treated with rotenone, an inhibitor of the respiratory chain in mitochondria, there was no effect on the superoxide production. Although DPI may inhibit enzymes other than NADPH oxidase, it is likely that neutrophil-like keratinocytic NADPH oxidase produces a major portion of the superoxide generated. It is unlikely that the superoxide comes from mitochondria. We hypothesize that dominant activated ras transduction somehow activates keratinocyte NADPH oxidase.

ras proteins are associated with the plasma membrane, and this is essential for their biological functions. Membrane association is caused by a series of post-translational modifications of p21<sup>ras</sup>. The first and obligatory step for its transforming activity consists of the covalent binding of a polyisoprenoid, a farnesyl group, to the system residue located in the COOH-terminus tetrapeptide, in a reaction catalyzed by farnesyl protein transferase [22]. D19 cells were treated for 48 h with 100  $\mu$ M lovastatin, an inhibitor of farnesyl synthesis that inhibits ras protein maturation. The cytochrome c assay showed attenuation of cytochrome c reduction; this observation suggested that O<sub>2</sub><sup>-</sup> generation in D19 cells was dependent on oncogenic ras.

To prevent oxidative damage and allow survival in an oxygen environment, mammalian cells have developed an elaborate antioxidant defense system that includes MnSOD and CuZnSOD, both of which are scavengers of superoxide that form H<sub>2</sub>O<sub>2</sub>. Previous work [5] and the study reported here showed that extracellular SOD protein could lower the superoxide production induced by ras. However, extracellular SOD protein cannot enter most cells, and thus these experiments indicated production of the extracellular O<sub>2</sub><sup>-</sup>. No one has investigated whether intracellular SOD lowers O<sub>2</sub><sup>-</sup> levels. To test whether intracellular SOD gene transfection can modify O<sub>2</sub><sup>-</sup> generation, we used replication-defective recombinant adenoviral vectors to transduce human *MnSOD*, *CuZnSOD*, and *CAT* genes into D19 cells; at the same time, an adenoviral vector-transduced bacterial *lacZ* gene was used as a control. Adenovirus constructs have been shown in our lab to very effectively deliver and express *MnSOD* cDNA in oral cancer cells [24]. Our experiments showed that both MnSOD and CuZnSOD protein levels and activity could be elevated by this gene overexpression in D19 cells. Compared with D19 or Ad*LacZ*-transformed D19 cells, in cells transfected with human *MnSOD* or *CuZnSOD* cDNA but not *CAT* cDNA, the O<sub>2</sub><sup>-</sup> generation was modified. The degree of modification seemed a little higher for the *CuZnSOD* gene than for the *MnSOD* gene (Figure 4), but this difference was not statistically significant ( $P > 0.05$ ). Although CuZnSOD protein is located in the cytosol and MnSOD is located in the

mitochondrial matrix, they have the similar effects. CAT, which converts H<sub>2</sub>O<sub>2</sub> to H<sub>2</sub>O, had almost no effect on modification of O<sub>2</sub><sup>-</sup> generation. These experiments demonstrated for the first time production of intracellular O<sub>2</sub><sup>-</sup> induced by ras.

Superoxide may act as a second-messenger signaling molecule. When fibroblast cells are transformed by mutant oncogenic ras, a larger amount of superoxide production is detected in the transformed cells than the parental cells and Neo cells, and the transformed cells proliferate faster [5]. Dr. Bar-Sagi's lab also found that Rac-induced superoxide production is a critical mediator of mitogenic signaling [25]. Dr. Finkel's lab demonstrated that V12Ras expression in primary human diploid fibroblasts induces senescence by altering the intracellular levels of ROS [26]; more importantly, their data demonstrated that the simultaneous expression of V12Rac1 results in an increase in cell growth compared with V12Ras expression alone. The mechanism could be the same as for ras: V12Rac1 may induce superoxide production by activating its NADPH oxidase, and superoxide promotes cell growth. In the study reported here, we found that v-Ha-ras-transformed HaCaT keratinocytes had increased production of superoxide radical compared with vector control cells and the parental HaCaT cells. Approximately 30% of all human tumors have *ras* mutations, which implies that superoxide production may be increased in these cells. However, cancer cells express low, constitutive level of MnSOD and CuZnSOD when compared with their cells of origin [27], which suggests that cancer cells may take advantage of their superoxide production to accelerate growth. Because less O<sub>2</sub><sup>-</sup> is scavenged by MnSOD and CuZnSOD, tumor cells can maintain a relatively high level of O<sub>2</sub><sup>-</sup>, which may act as a mediator of mitogenic signals. We therefore propose that constitutive production of superoxide in ras-transformed D19 cells activates intracellular pathways that may promote cell proliferation. The identification of the molecular targets of this pathway will provide insights into the mechanisms linking superoxide and growth control.

#### ACKNOWLEDGMENTS

We gratefully thank Weiling Zhao for RT-PCR and Sean Martin for EPR technical help. This work was supported by NIH grants P50-DE10758 and P01-CA 66081.

#### REFERENCES

1. Henderson LM, Chappell JB. NADPH oxidase of neutrophils. *Biochem Biophys Acta* 1996;1273:87-107.
2. Prigmore E, Ahmed S, Best A, et al. A 68-kDa kinase and NADPH oxidase component p68phox are targets for Cdc42Hs and Rac1 in neutrophils. *J Biol Chem* 1995;270:10717-10722.

3. Turner CP, Toye AM, Jones OTG. Keratinocyte superoxide generation. *Free Radic Biol Med* 1997;24:401–407.
4. Sundaresan M, Yu Z, Ferrans VJ, et al. Regulation of reactive-oxygen-species generation in fibroblasts by Rac 1. *Biochem J* 1996;318:379–382.
5. Irani K, Xia Y, Zweier JL, et al. Mitogenic signaling mediated by oxidants in Ras-transformed fibroblasts. *Science* 1997;275:1649–1651.
6. Pagano PJ, Clark JK, Cifuentes-Pagano ME, Clark SM, Callis GM, Quinn MT. Localization of a constitutively active, phagocyte-like NADPH oxidase in rabbit aortic adventitia: Enhancement by angiotensin II. *Proc Natl Acad Sci USA* 1997;94:14483–14488.
7. Oberley LW, Oberley TD. Role of antioxidant enzymes in the cancer cell phenotype. In: Clerch LB, Massaro DJ, editors. *Oxygen, gene expression, and cellular function*. New York: Marcel Dekker, Inc., 1997. p 279–307.
8. Guyton KZ, Liu Y, Gorospe M, Xu Q, Holbrook NJ. Activation of mitogen-activated protein kinase by H<sub>2</sub>O<sub>2</sub>. Role in cell survival following oxidant injury. *J Biol Chem* 1996;271:4138–4142.
9. Sundaresan M, Yu Z, Ferrans VJ, Irani K, Finkel T. Requirement for generation of H<sub>2</sub>O<sub>2</sub> for platelet-derived growth factor signal transduction. *Science* 1995;270:296–299.
10. Bhunia AK, Han H, Snowden A, Chatterjee S. Redox-regulated signaling by lactosylceramide in the proliferation of human aortic smooth muscle cells. *J Biol Chem* 1997;272:15642–15649.
11. Pai EF, Kabsch W, Kregel U, Holmes KC, John J, Wittinghofer A. Structure of the guanine-nucleotide-binding domain of the Ha-ras oncogene product p21 in the triphosphate conformation. *Nature* 1989;341:209–214.
12. Lowy DR, Willumsen BM. Function and regulation of ras. *Annu Rev Biochem* 1993;62:851–891.
13. Boukamp P, Petrussevska RT, Breitkreutz D, Hornung J, Markham A, Fusenig NE. Normal keratinization in a spontaneously immortalized aneuploid human keratinocyte cell line. *J Cell Biol* 1988;106:761–771.
14. Wang BC, Kennan WS, Yasukawa-Barnes J, Lindstrom MJ, Gould MN. Carcinoma induction following direct in situ transfer of v-Ha-ras into rat mammary epithelial cells using replication-defective retrovirus vectors. *Cancer Res* 1991;51:2642–2648.
15. Spitz DR, Elwell JH, Sun Y, et al. Oxygen toxicity in control and H<sub>2</sub>O<sub>2</sub>-resistant Chinese hamster fibroblast cell lines. *Archives Biochem Biophys* 1990;279:249–260.
16. Buettner GR. In the absence of catalytic metals ascorbate does not autoxidize at pH 7: Ascorbate as a test for catalytic metals. *J Biochem Biophys Methods* 1988;16:27–40.
17. Butler J, Koppenol WH, Margoliash E. Kinetics and mechanism of the reduction of ferricytochrome c by the superoxide anion. *J Biol Chem* 1982;257:10747–10750.
18. Wang Q, Finer MH. Second-generation adenovirus vectors. *Nature Med* 1996;2:714–716.
19. Zwacka RM, Dudus L, Epperly MW, Greenberger JS, Engelhardt JF. Redox gene therapy protects human IB-3 lung epithelial cells against ionizing radiation-induced apoptosis. *Human Gene Therapy* 1998;9:1381–1386.
20. Heldman AW, Kandzer DE, Tucker RW, et al. EJ-Ras inhibits phospholipase C $\gamma_1$  but not actin polymerization induced by platelet-derived growth factor-BB via phosphatidylinositol 3-kinase. *Circulation Res* 1996;78:312–321.
21. Buettner GR. Spin trapping: ESR parameters of spin adducts. *Free Radic Biol Med* 1987;3:259–303.
22. Rosen GM, Freeman BA. Detection of superoxide generated by endothelial cells. *Proc Natl Acad Sci USA* 1984;81:7269–7273.
23. Santillo M, Mondola P, Gioielli A, et al. Inhibitors of Ras farnesylation revert the increased resistance to oxidative stress in K-ras transformed NIH 3T3 cells. *Biochem Biophys Res Comm* 1996;229:739–745.
24. Lam E, Zwacka R, Engelhardt JF, et al. Adenovirus-mediated manganese superoxide dismutase gene transfer to hamster cheek pouch carcinoma cells. *Cancer Res* 1997;57:5550–5556.
25. Joneson T, Bar-Sagi D. A Rac1 effector site controlling mitogenesis through superoxide production. *J Biol Chem* 1998;273:17991–17994.
26. Lee AC, Fenster BE, Ito F, et al. Ras proteins induce senescence by altering the intracellular levels of reactive oxygen species. *J Biol Chem* 1999;274:7936–7940.
27. Oberley LW, Buettner GR. Role of superoxide dismutase in cancer: A review. *Cancer Res* 1979;39:1131–1149.